physica status solidi

pss

www.pss-journals.com

reprint

WILEY-VCH

Phys. Status Solidi C **10**, No. 11, 1353–1356 (2013) / **DOI** 10.1002/pssc.201300255

physica status solidi c
www.pss-c.com
current topics in solid state physics

High growth rates of AlN and AlGaN on 8” silicon wafer using metal-organic vapor phase epitaxy reactor

Akinori Ubukata[*, 1], Yoshiki Yano[1], Yuya Yamaoka[1], Yuichiro Kitamura[1], Toshiya Tabuchi[1], and Koh Matsumoto[2]

[1] Taiyo Nippon Sanso Corporation, 10 Ohkubo, Tsukuba, Ibaraki 300-2611, Japan
[2] TN EMC Ltd., 2008-2 Wada, Tama-shi, Tokyo 206-0001, Japan

Received 22 June 2013, revised 21 August 2013, accepted 28 August 2013
Published online 23 October 2013

Keywords AlN, mass transfer, metal-organic vapor phase epitaxy

[*] Corresponding author: e-mail Akinori.Ubukata@tn-sanso.co.jp

We have developed a large-scale metal-organic vapor phase epitaxy (MOVPE) reactor. The growth rates of AlN and AlGaN were compared with those calculated using the parasitic chemical reaction model. The calculated results were in good agreement with the experimental results over the entire 8” wafer. To experimentally investigate the extent of the gas-phase prereaction between the precursors and ammonia, the results of epitaxy were compared with those for a 6”-type reactor. The growth of AlN and AlGaN at relatively high rates without any significant gas-phase prereaction was demonstrated.

1 Introduction

There has been considerable interest in the growth of GaN on Si since GaN is the most important semiconductor next to silicon because of its applications in solid-state lighting and high-power switching devices [1]. Outstanding GaN power devices that break the silicon limit have been demonstrated by various groups [2-7]. To reduce the manufacturing cost of GaN power devices, the GaN-on-Si approach has attracted industrial attention because silicon substrates are inexpensive, available in large sizes and can also be readily applied to conventional production lines for GaAs or Si devices. A problem remaining in the growth of AlN or AlGaN is a gas-phase prereaction that occurs between trimethylaluminum (TMA) and ammonia rather than with other precursor materials [8]. This prereaction readily occurs at high TMA and ammonia flow rates or at a high growth pressure, which leads to a considerable reduction in the growth rate and Al composition in solid AlGaN. The use of a large high-throughput reactor has contributed to the reduction in wafer cost; however, the low growth rate due to the effect of the gas-phase prereaction remains an issue.

In this study, a large-scale metal-oraganic vapour-phase epitaxy (MOVPE) reactor was developed, which can be used to grow AlN and AlGaN on 8” wafers. We applied the parasitic vapor reaction model to this large-scale reactor to study the effect of the gas-phase prereaction. The experimental growth of AlN and AlGaN was performed and compared with the result of modeling.

2 Modeling the parasitic vapor reaction

Computational fluid dynamic (CFD) simulations considering gas-phase chemical reactions and surface chemistry were carried out to study their effect on the growth rate. This numerical approach can predict the growth rate of AlN and the deposition rate on the reactor components using CVD-Sim software (STR Group, Inc.) with modified FLUENT software to model the coupled fluid flow, species transport, gas phase chemistry and surface chemistry in a laminar-flow-type MOVPE reactor. It was also necessary to consider the effect of the transport of particulate species, which are generated in the gas phase and decrease the growth rate of films. The quasi-thermodynamic (QT) mechanism describes the chemical reactions of the input species, i.e., trimethylgallium (TMG), TMA and ammonia, which result in the film growth, as well as the formation of gas-phase particulates. The governing equations are three-dimensional and assume a vapor-phase chemical reaction, which is described in a previous report [9]. The growth rate is determined by the adhesion coefficient, which depends

on the temperature, implying the dependence of the growth rate on the supply of adduct species. The temperature dependence of each reaction rate constant is given in Arrhenius form. The particulates generated in the vapor phase are a cause of material loss. Using this model, we predicted the effect of the gas-phase reaction from the obtained growth rate. In the model, we assume the use of a planetary-type multiwafer 8”-type reactor with a capacity of 6 × 8”. The model was solved by considering two-dimensional (2D) cross sections surrounding the growth region.

Figure 1 shows the cross-sectional distribution of the Al adduct as a function of the total carrier gas flow rate in the reactor. The standard total carrier flow rate of our reactor is denoted as “Std flow” in Fig. 1. The gas injection nozzle is on the left side of the figure, and the region between the dashed white lines is the 8” wafer zone. The sequence of reactions between TMA and NH_3 results in adduct formation at a low temperature, and the reaction rate is considerably high. Upon heating, the $Al(CH_3)_3$:NH_3 adduct may decompose to $Al(CH_3)_2$:NH_2 in a parallel reaction, resulting in the elimination of methane. This reaction is different from that of the Ga adduct because the initial Ga adduct decomposes in a backward reaction to produce TMG and NH_3. This specific feature makes Al-related parasitic reactions more intensive than the GaN reaction and may result in the further formation of AlN nanoparticles.

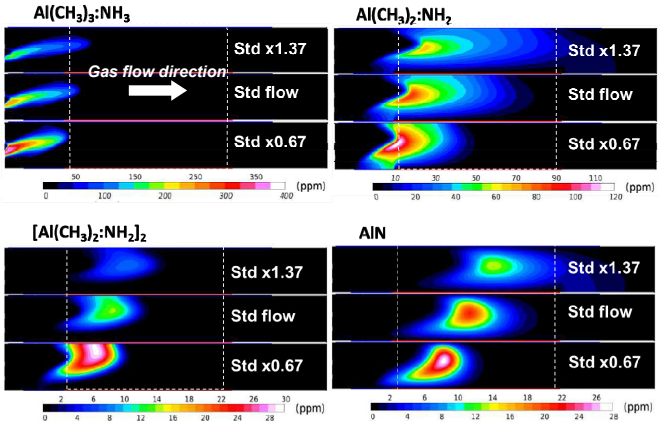

Figure 1 Distribution of Al adduct as a function of total carrier flow rate.

3 Experimental procedure and results

The growth of AlN and AlGaN was performed in a large-scale reactor (Taiyo Nippon Sanso Co., UR26K) used for the manufacture of LEDs and electron devices, which has a capacity of 10×6” or 6×8”. Wafers are rotated by planetary motion using mechanical gears so that each rotation speed is constant. Briefly, the precursors are supplied from the bottom of the reactor and then injected into the reaction zone from a trilayer nozzle at the center of the reactor. The injection nozzle is designed to produce a high flow speed, enabling the suppression of undesirable parasitic reactions in the vapor phase without causing turbulence. TMG, TMA and ammonia were used as the source gases of Ga, Al and N, respectively. Ammonia, N_2 and H_2 were introduced from bottom side of the injection nozzle. The precursors and N_2 and H_2 were introduced from the middle side, and only N_2 was introduced from the top side. The H_2 concentration in the N_2/H_2 mixture was kept constant throughout this experiment. The design criteria of the reactor were described in a previous paper [10].

Figure 2 shows a comparison of the growth rate of AlN obtained from the QT model and experimental data obtained using a non-satellite rotation wafer holder as a function of the total carrier gas flow rate. The growth temperature and growth pressure were 1080 °C and 15 kPa, respectively. One of the most common features of the Al(Ga)N MOVPE process is the reduction in the total growth rate that occurs in the case of a significant gas-phase prereaction between TMA and ammonia. At a lower carrier gas flow rate than the standard condition, there is a significant reduction in the growth rate, which is almost zero in the middle of the wafer. This is due to particulate generation in the gas phase. Thus, the standard flow rate or higher is required for the carrier gas to suppress this effect. With increasing total carrier flow rate, the peak of the growth rate shifted downstream and the maximum growth rate decreased.

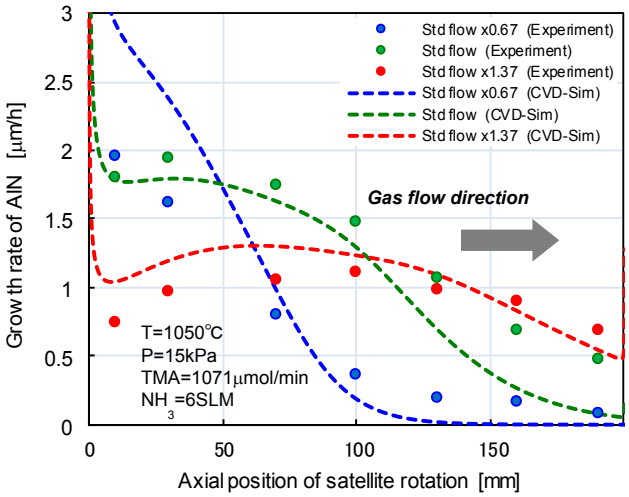

Figure 2 Growth rate of AlN as a function of total carrier gas flow rate.

Figure 3 shows the AlN growth rate on an 8” wafer without satellite rotation as a function of the top-side flow rate. As described in a previous report, the thickness uniformity can be controlled by balancing the carrier flow balance [11]. The growth rate upstream of the 8” wafer was affected by the carrier flow balance, which is a result of the suppression of the stagnant layer. The deposition rates on the reactor components such as the sealing plates and susceptor were also determined. When the top-side flow rate was twice the other flow rates (2:1:1), the thickness uniformity of AlN was 1.1% with satellite rotation. We found that the deposition on the reactor components can be controlled by balancing the carrier flow rates.

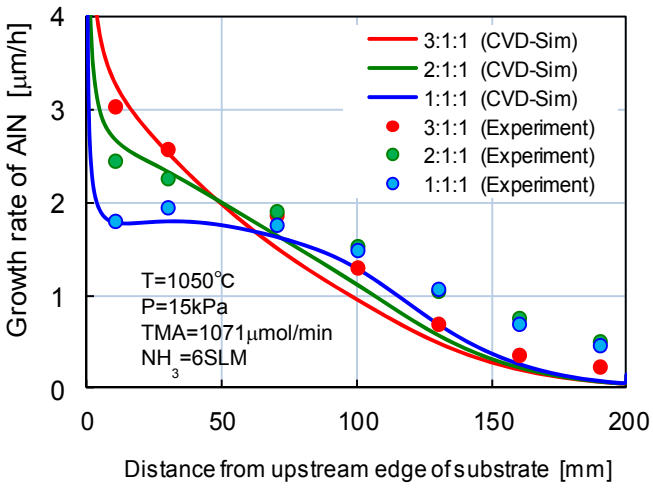

Figure 3 Growth rate of AlN as a function of carrier gas balance.

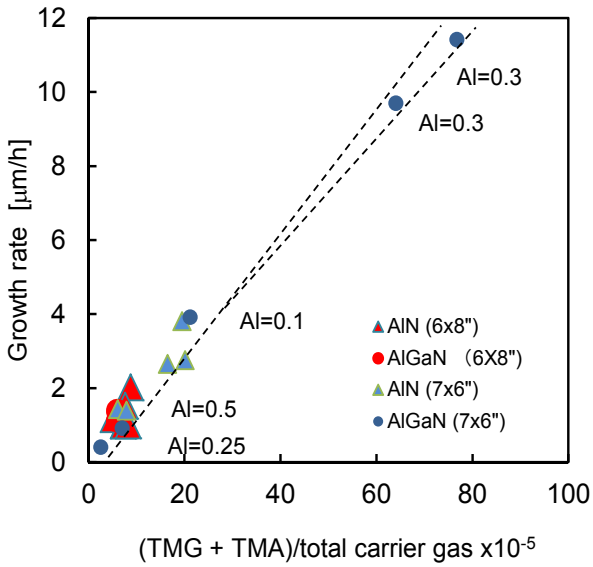

Figure 4 Growth rates of AlN and AlGaN as a function of precursor input.

Next, the experimental results were compared with those obtained using another planetary-type reactor with a capacity of 7×6" [12]. The dimensions of the growth region and the materials, such as the height of the gas-flow region, the distance from the injection nozzle and the materials of the reactor components, are the same as those for the experimental 6×8" reactor. Thus, the distribution of the Al adduct can be expected to be almost the same for both reactors. Figure 4 shows the growth rates of AlN and AlGaN as a function of the precursor input normalized by the total carrier gas flow rate using these reactors. The ammonia flow rate was kept constant at 6 SLM, while V/III was reduced during the increase in TMA input. The growth rate of AlN increased linearly, close to the transport limit. The growth rate of AlGaN with various Al compositions is also plotted, which increased linearly or changed slightly with the precursor input. This change can be explained as a shift in the equilibrium of the reaction of $Al(CH_3)_3$:NH_3 to form TMA:NH_3, which generates heavy dimers such as $[Al(CH_3)_2{:}NH_2]_2$ and is followed by the formation of particles in the gas phase. However, the effect of these heavy dimers is not significant in the range of growth rates considered here. Maximum growth rates of 4 μm/h and 11 μm/h were obtained for AlN and $Al_{0.3}Ga_{0.7}N$, respectively. The thickness and composition uniformities were less than 2% and 0.001 even at a growth rate of 11 μm/h, respectively. A higher growth rate can be obtained by extending the mass flow controller of TMA because the maximum growth rate was limited by the TMA supply.

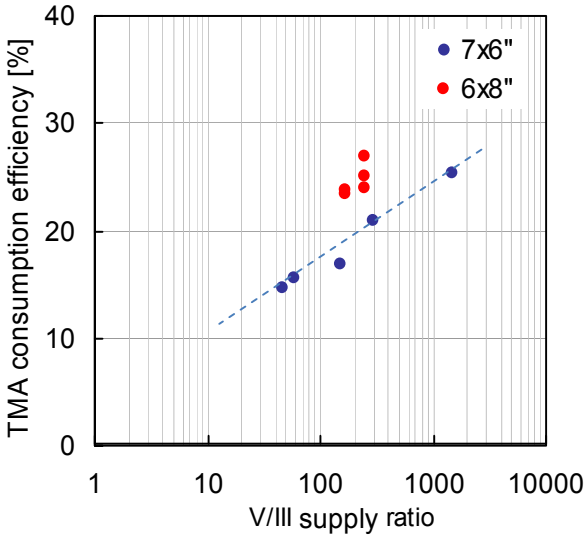

Figure 5 TMA consumption efficiency of AlN as a function of TMA input.

Figure 5 shows the V/III supply ratio dependence of the TMA consumption efficiency of AlN. If a relatively low flow velocity is employed, an increase in the ammonia flow rate should result in a slight reduction of the growth rate, which can be explained by the almost complete conversion of TMA into the adduct. In this experiment, a relatively high flow velocity was employed; the growth efficiency was not saturated even at a V/III ratio of 1000, and the consumption efficiency continued to increase above this V/III ratio. This result corresponds to the equilibrium

in the primitive adduct reaction from $Al(CH_3)_3$:NH_3 to TMA:NH_3, meaning that the amount of ammonia can be increased without the formation of particles in the gas phase.

As AlN and AlGaN are the dominant materials in AlGaN/GaN electronic device structures, increasing the high-rate growth of AlN or AlGaN is a means of improving the throughput. Figure 6 shows the thickness uniformity of a 3.7-μm-thick AlGaN/GaN high-electron-mobility transistor (HEMT) structure on 8” Si substrates. The structure consists of a 400-nm-thick AlGaN/AlN buffer layer, a 2.6-μm-thick (AlGaN/AlN) superlattice structure (SLS) and a 700-nm-thick GaN buffer layer. In this device, over 80% of the structure consists of Al-related materials to control the wafer curvature and lattice constant. The thickness uniformity (1-σ) of each wafer was in the range from 1.5% to 1.8%. The thickness and Al composition were affected by the wafer curvature during the growth. This issue will be discussed in a future work. The total thickness variation of the six wafers was Δ = 0.9%. The average growth rate of the SLS was 2.8 μm/h. By applying our technique with the higher growth rate, the epi layer was fabricated in less than 4 h including standby time and ramping/cooling time. This is important for obtaining a high throughput.

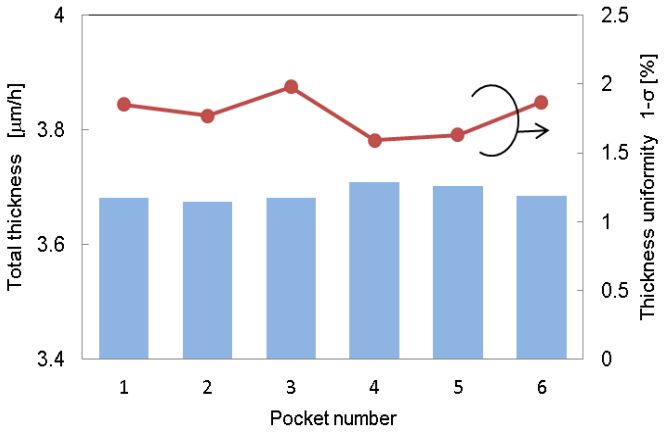

Figure 6 Thickness uniformity of AlGaN/GaN HEMT structure on 8” Si.

We also have found that an increase in surface roughness is correlated with an increase in the growth rate. Surface defects can induce a high reverse gate leakage current in devices [13]. The roughness (RMS) of the sample grown at 11 μm/h was 1.4 nm according to the results of AFM measurement, while that of samples grown at 1 μm/h was approximately 0.4 nm. Some groups have reported the introduction of a surfactant such as TMI [14], the doping of a small amount of Ga [15] or the use of a quasi-AlGaN barrier [16] to improve the surface roughness. A future investigation of this issue will be reported elsewhere.

4 Conclusion

The fluid dynamics of a 6×8” MOVPE reactor was modeled. The growth rate derived from the QT model at a high velocity was closely fitted with the experimentally observed AlN epitaxial growth rate. This indicates that the prereaction in the gas phase does not have a significant effect in this reactor. Also the growth rates of AlN and AlGaN were experimentally compared with those in another reactor, and a high growth rate was demonstrated for our MOVPE reactor.

References

[1] C. Jun, Z. Shuming, Z. Baoshun, Z. Jianjun, F. Gan, D. Lihong, W. Yutian, Y. Hui, and Z. Wenchen, Sci. Chin., Ser. E **46**, 620 (2003).

[2] Y. Uemoto, T. Morita, A. Ikoshi, H. Ueda, H. Matsuo, J. Shimizu, M. Hikita, M. Yanagihara, T. Ueda, T. Tanaka, and D. Ueda, IEDM Tech. Dig. 1 (2009).

[3] N. Ikeda, Y. Niiyama, H. Kambayashi, Y. Satoh, T. Nomura, S. Kato, and S. Yoshida, Proc. IEEE **98**, 1151 (2010).

[4] Y. Dora, A. Chakraborty, L. McCarthy, S. Keller, S. P. DenBaars, and U. K. Mishra, IEEE Electron Device Lett. **27**, 713 (2006).

[5] A. R. Boyd, S. Degroote, M. Leys, F. Schulte, O. Rockenfeller, M. Luenenbuerger, M. Germain, J. Kaeppeler, and M. Heuken, Phys. Status Solidi C **6**, s1045 (2009).

[6] J. Li, J. Y. Lin, and H. X. Jiang,Appl. Phys. Lett. **88**, 171909 (2006).

[7] K. Matsumoto and A. Tachibana, J. Cryst. Growth **272**, 360 (2004).

[8] T. Tokunaga, Y. Fukuda, A. Ubukata, K. Ikenaga, Y. Inaishi, T. Orita, S. Hasaka, Y. Kitamura, A. Yamaguchi, S. Koseki, K. Uematsu, N. Tomita, N. Akutsu, and K. Matsumoto, Phys. Status Solidi C **5**, 3017 (2008).

[9] A. V. Lobanova, K. M. Mazaev, R. A Talalaev, M. Leys, S. Boeykens, K. Cheng, S. Degroote, J. Cryst. Growth **287**, 601 (2006).

[10] S. Nicolay, E. Feltin, J.-F. Carlin, M. Mosca, L. Nevou, M. Tchernycheva, F. H. Julien, M. Ilegems, and N. Grandjean, Appl. Phys. Lett. **88**, 151902 (2006).

[11] Y. Yano, H. Tokunaga, H. Shimamura, Y. Yamaoka, A. Ubukata, T. Tabuchi, and K. Matsumoto, Jpn. J. Appl. Phys. **52**, 08JB06 (2013).

[12] A. Ubukata, Y. Yano, H. Shimamura, A. Yamaguchi, T. Tabuchi, and K. Matsumoto, J. Cryst. Growth **370**, 269 (2013).

[13] Y. Zhou, R. Chu, J. Liu, K. J. Chen, and K. M. Lau, Phys. Status Solidi C **2**, 2663 (2005).

[14] X. Zhu, J. Ma, T. Huang, M. Li, K. M. Wong, and K. M. Lau, Phys. Status Solidi C **9**, 473 (2012).

[15] W. V. Lundin, A. E. Nikolaev, M. A. Yagovkina, P. N. Brunkov, M. M. Rozhavskaya, B. Ya. Ber, D. Yu. Kazantsev, A. F. Tsatsulnikov, A. V. Lobanova, and R. A. Talaev, J. Cryst. Growth **352**, 209 (2012).

[16] Y. Kawakami, X. Q. Shen, G. Piao, M. Shimizu, H. Nakanishi, and H. Okumura, J. Cryst. Growth **300**, 168 (2007).

